A Photoinduced Mixed-Valence State in an Organic Bis-Triarylamine Mixed-Valence Compound with an Iridium-Metal-Bridge

Christoph Lambert*, Reinhard Wagener, Johannes H. Klein, Guillaume Grelaud, Michael Moos, Alexander Schmiedel, Marco Holzapfel, Torsten Bruhn

Institut für Organische Chemie, Center for Nanosystems Chemistry,

Universität Würzburg, Am Hubland, 97074 Würzburg, Germany

A. Synthesis

1. Generalities

All reactions were carried-out under an atmosphere of nitrogen (dried with Sicapent from Merck, oxygen was removed with a cupric oxide catalyst R3-11 from BASF) using standard Schlenk techniques.[1] Solvent for oxygen and/or moisture sensitive reactions were freshly distilled under nitrogen from the appropriate dehydrating agent (sodium for toluene, sodium/benzophenone "ketyl blue" for THF and CaH_2 for CH_2Cl_2 and MeCN) and sparged with dry nitrogen before use. Solvents for chromatography and work-up procedures were of technical grade and distilled by direct distillation prior to use. Deuterated solvents were used as received. Flash chromatography[2] was performed on silica gel (Macherey-Nagel "Silica 60 M", 40 – 63 μm) wet-packed in glass column of size indicated as diameter x length. Gel permeation chromatography (GPC) was done using a Jasco recycling GPC/HPLC-system with two preparative GPC columns (styrene-divinylbenzene-copolymer, 50 and 500 Å, 600 x 20.8 mm) from PSS, a four channel UV/vis-detector (195 – 700 nm) and a fraction collector. The flow rate was 4 ml·min^{-1}. Silica plates (Merck $60F_{254}$) were used for thin layer chromatography (TLC) and revealed using an UV lamp (254 nm, 365 nm for fluorescent compounds) or chemical stains (vanillin, $KMnO_4$ or silica-adsorbed iodine), if necessary.

2. Instrumentation

^1H and ^{13}C NMR spectra were acquired on a Bruker Avance 400-FT-spectrometer (^1H at 400.1 MHz, ^{13}C at 100.6 MHz) at 300 K in acetone-d_6 or chloroform-*d.* Some spectra were also recorded on a Bruker AVANCE 600 DMX FT spectrometer (^1H at 600.1 MHz, ^{13}C at 150.9 MHz) at 298.8 K for acetone-d_6 or 303.6 K for chloroform-*d*. Samples were filtered and placed in frequency-matched 5 mm glass sample tubes. Chemical shifts are given in ppm relative to residual nondeuterated solvent signal (^1H: $CHCl_3$: δ 7.26 ppm, acetone: δ 2.05 ppm; ^{13}C: $CHCl_3$: δ 77.2 ppm, acetone: δ 29.8 ppm).[3] Multiplet signals or overlapping multiplet signals in proton NMR spectra that could not be assigned to first order couplings are given as (-). Mass spectra were recorded with a Bruker Daltonics autoflex II (MALDI) in positive mode (POS) using a DCTB (*trans*-2-[3-(4-*tert*-butylphenyl)-2-methyl-2-propenylidene]malononitrile) matrix or with a Bruker Daltonic microTOF focus (ESI). All mass spectrometry peaks are reported as m/z. Elemental analyses were performed with a vario Micro CHNS from elementar at the Institute of Inorganic Chemistry, University of Würzburg.

3. Reagents

4-Bromo-*N*,*N*-*bis*(4-methoxyphenyl)aniline[4], **(3)** *meso*-phenyldipyrromethane[5] **(4)**, *meso*-(4-(*N*-(2,5-di-*tert*-butylphenyl)-naphthalene-1,4,5,8-tetracarboxyldiimide)phenyl)dipyrromethane[6] **(5)** and (*N*-(2,5-di-*tert*-butylphenyl)-naphthalene-1,4,5,8-tetracarboxyldiimide)benzene[6] **(6)** were prepared according to the corresponding literature procedures. 4-iodoanisole and 1*H*-pyrazole were recrystallised from hexanes, salicylaldoxime was recrystallised from CH_2Cl_2/hexanes and 2,3-dichloro-5,6-dicyano-1,4-benzoquinone (DDQ) from $CHCl_3$. All other reagents were used as received.

4. Procedures

4.1 Overview of the synthesis

The starting bromo-*N,N*-*bis*(4-methoxyphenyl)anilines[7] **(3, 7)** were prepared from the corresponding commercially available bromoanilines, by Ullman coupling with 4-iodoanisole under the conditions reported by Wenger and his co-workers.[4] In the following step, a copper-catalysed *N*-arylation of pyrazole[8] afforded the desired *N*,*N*-*bis*(4-methoxyphenyl)-substituted phenylpyrazole cyclometalating ligands **(8, 9)** (Scheme S1).

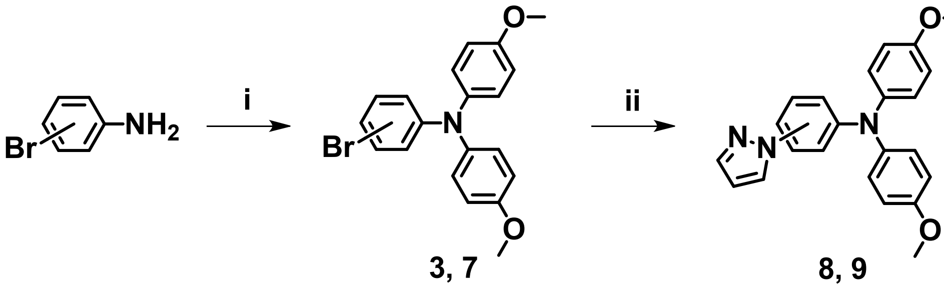

Scheme S1 : Reagents and conditions: i) 4-iodoanisole (2.2 eq.), 1,10-phenanthroline (5 mol %), CuI (5 mol %), KOH (10 eq.), toluene, 120 °C, 72 h; **3**: 78 %, **7**: 57 %[4]; ii) 1-*H*-pyrazole (1.5 eq.), Cu_2O (5 mol %) salicylaldoxime (20 mol %), Cs_2CO_3 (2.1 eq.), MeCN, 80 °C, 72 h; **8**: 91 %, **9**: 65 %.

The syntheses of the *bis*-cyclometalated dipyrrinato iridium complexes **(2p, 2m, 1p, 1m)** were achieved following the general method reported by Thompson *et al.*[9] First the *N*,*N*-*bis*(4-methoxyphenyl)-substituted phenylpyrazole cyclometalating ligands **(8, 9)** were treated with iridium(III) chloride under the Nomoyama[10] route to give the *μ*-Cl bridged dimer **(10, 11)** which were further treated with the appropiate dipyrrin ligand **(5, 6)** in presence of K_2CO_3, *in-situ* generated by oxidation of the dipyrromethane with DDQ (Scheme S2).

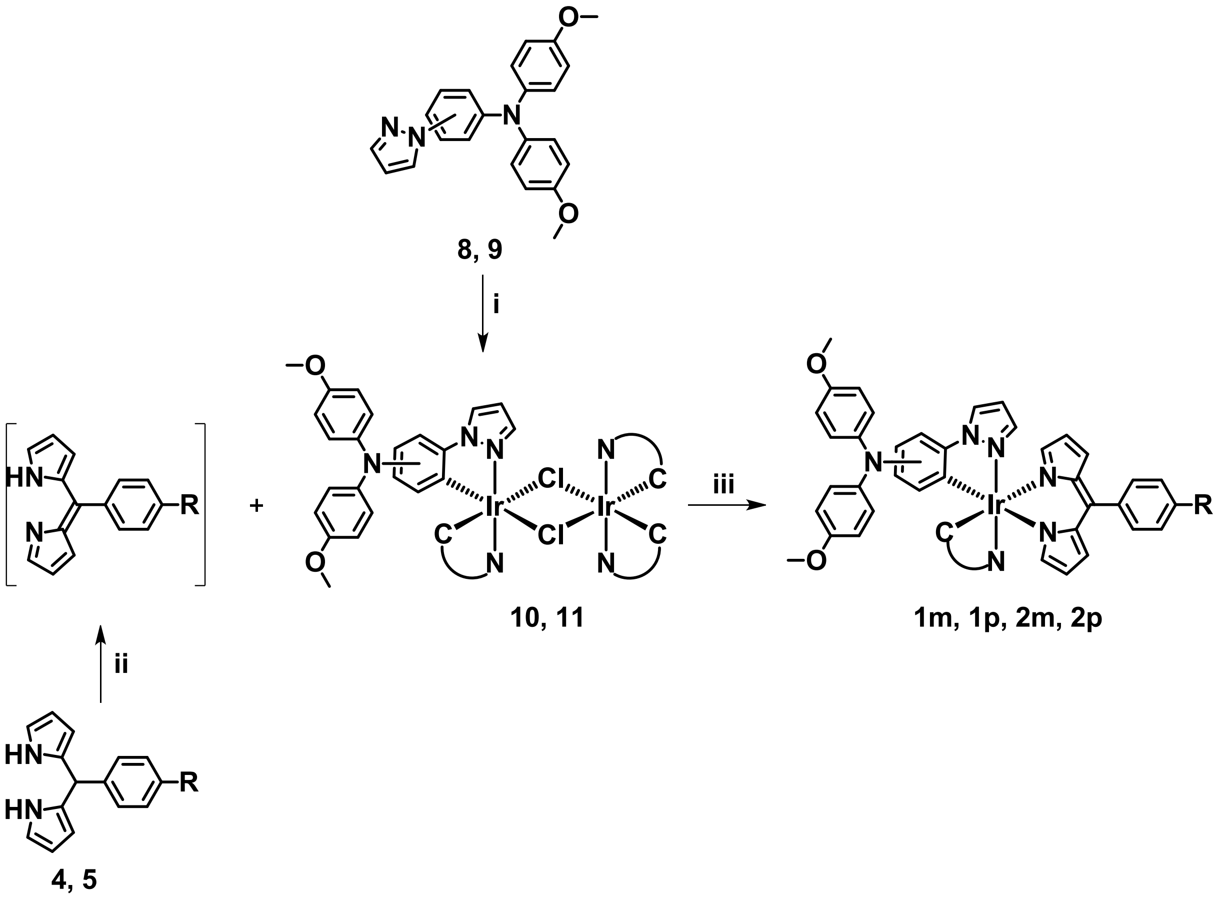

Scheme S2: Reagents and conditions: i) $IrCl_3{\cdot}3H_2O$ (0.50 eq.), 2-ethoxyethanol/water 3:1, 100 °C, 24 h; **10** quant., **11** quant.; ii) DDQ (1.0 eq., 1 h: **4,** 1.1 eq., 3 h: **5**); iii) excess K_2CO_3, THF, 60 °C (**4**) or reflux (**5**); **2p:** 87 %, **2m:** 91 %, **1p:** 29 %, **1m:** 62 %.

4.2 3-Bromo-*N,N*-*bis*(4-methoxyphenyl)aniline (7)[7]

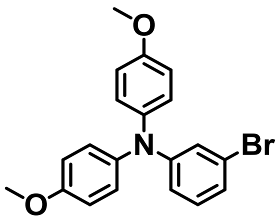

$C_{20}H_{18}BrNO_2$, M = 384.27 g/mol

4-Iodoanisole (5.15 g, 22.0 mmol), copper iodide (0.095 g, 0.50 mmol), 1,10-phenanthroline (0.090 g, 0.50 mmol) and finely powdered potassium hydroxide (5.61 g, 100.0 mmol) were suspended in dry toluene (10 mL) and sparged with nitrogen for 5 min. Then 3-bromoaniline (1.72 g, 10.0 mmol) was added and the heterogeneous mixture was heated at 120 °C for 72 h. The reaction mixture was cooled down to room temperature, hydrolysed with water (50 mL) and extracted with CH_2Cl_2 (3 x 50 mL). The combined organic extracts were washed with 10 % aqueous HCl, water, saturated aqueous $NaHCO_3$, water and saturated aqueous NaCl (50 mL each), dried ($MgSO_4$) and solvents removed under reduced pressure. The crude dark-brown oil was adsorbed onto celite and purified by column chromatography (silica gel, 5 x 25 cm) using hexanes/ethyl acetate 15:1 as the eluent. The fractions containing the pure desired compound were collected, combined and taken to dryness by rotary evaporation. The resulting colourless oil was dried *in vacuo* until it has fully crystallised; the solid mass was then reduced to a fine white powder with a spatula and further dried *in vacuo* (3.01 g, 7.83 mmol, 78 %).

R_f (hexanes/ethyl acetate 15:1): 0.45.

mp: 81 - 83 °C.

Maldi-TOF (POS, DCTB/$CHCl_3$ 1:3): calc: 383.052 $[M]^+$, found: 383.025.

^{1}H NMR (400.1 MHz, chloroform-*d*, ppm): δ 7.05 (AA‘, 4 H), 7.01 (-, 1 H), 6.98 (d, $^3J_{HH}$ = 7.9 Hz, 1 H), 6.93 (ddd, $^3J_{HH}$ = 7.8 Hz, $^4J_{HH}$ = 1.9 and 1.3 Hz, 1 H), 6.83 (BB‘, 4 H), 6.80 (ddd, $^3J_{HH}$ = 8.1 Hz, $^4J_{HH}$ = 2.3 and 1.2 Hz, 1 H), 3.80 (s, 6 H).

^{13}C NMR (100.6 MHz, chloroform-*d*, ppm): δ 153.5 (C_q), 150.43 (C_q), 140.37 (C_q), 130.2 (CH), 127.1 (CH), 122.95 (CH), 122.93 (C_q), 122.54 (CH), 118.45 (CH), 115.0 (CH), 55.6 (CH_3).

4.3 General procedure for the syntheses of (pyrazo-1-yl)-*N,N-bis*(4-methoxyphenyl)anilines from 1*H*-pyrazole and bromo-*N,N-bis*(4-methoxyphenyl)anilines

A mixture of the appropriate bromo-*N*,*N*-*bis*(*p*-methoxyphenyl)aniline (1.92 g, 5.0 mmol), 1*H*-pyrazole (0.51 g, 7.5 mmol), salicylaldoxime (0.137 g, 1.0 mmol), copper(I) oxide (0.036 g, 0.25 mmol) and cesium carbonate (3.42 g, 10.5 mmol) in dry MeCN (10 mL) was sparged with nitrogen for 5 min. The Schlenk flask was then sealed and the reaction mixture heated at 85 °C for 72 h. Once cooled to room temperature, the heterogeneous reaction mixture was diluted with ethyl acetate (25 mL), vigorously stirred for 5 min and then filtered through a small plug of celite (1 x 2 cm). The filter cake was washed with additional ethyl acetate (3 x 25 mL), the organic extracts were washed with saturated aqueous NH_4Cl, water and saturated aqueous NaCl (100 mL each). The aqueous layers were back-extracted with ethyl acetate (100 mL) and the second organic extract washed with water and saturated aqueous NaCl (100 mL each). The combined organic extracts were dried ($MgSO_4$) and taken to dryness on a rotavapor. The crude oil was purified by column chromatography followed by recrystallization, if applicable.

4.3.1 3-(pyrazo-1-yl)-*N*,*N*-*bis*(4-methoxyphenyl)aniline (8)

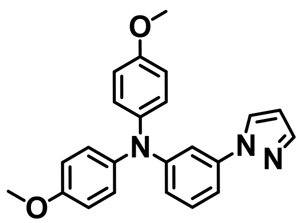

$C_{23}H_{21}N_3O_2$, M = 371.43 g/mol

From 3-bromo-*N*,*N*-*bis*(4-methoxyphenyl)aniline (1.92 g, 5.0 mmol), 1.70 g (4.58 mmol, 91 %) of colourless crystals were obtained after purification by column chromatography (silica gel, 4 x 25 cm) using hexanes/ethyl acetate 5:1 as the eluent, followed by recrystallisation from EtOH (60 mL) and water (40 mL). The crystals were washed with 50 % aqueous EtOH (10 mL) before being dried in *vacuo*.

R_f (hexanes/ethyl acetate 5:1): 0.38.

mp: 127 - 129 °C.

Maldi-TOF (POS, DCTB/$CHCl_3$ 1:3): calc: 371.163 $[M]^+$, found: 371.168.

^{1}H NMR (400.1 MHz, acetone-d_6, ppm): δ 8.12 (dd, $^{3}J_{HH}$ = 2.5 Hz, $^{4}J_{HH}$ = 0.6 Hz, 1 H), 7.57 (dd, $^{3}J_{HH}$ = 1.7 Hz, $^{4}J_{HH}$ = 0.5 Hz, 1 H), 7.38 - 7.36 (m, 1 H), 7.26 - 7.20 (-, 2 H), 7.10 (AA‘, 4 H), 6.91 (BB‘, 4 H), 6.71 (m, 1 H), 6.41 (dd, $^{3}J_{HH}$ = 2.6 and 1.8 Hz, 1 H), 3.78 (s, 6 H).

^{13}C NMR (100.6 MHz, acetone-d_6): δ 157.5 (C_q), 151.1 (C_q), 142.0 (C_q), 141.34 (CH), 141.32 (C_q), 130.7 (CH), 128.0 (CH), 127.7 (CH), 118.0 (CH), 115.8 (CH), 110.82 (CH), 110.75 (CH), 108.2 (CH), 55.7 (CH_3).

4.3.2 4-(pyrazo-1-yl)-*N,N*-*bis*(4-methoxyphenyl)aniline (9)

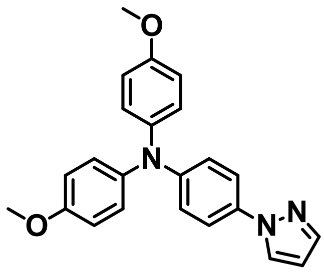

$C_{23}H_{21}N_3O_2$, M = 371.43 g/mol

From 4-bromo-*N*,*N*-*bis*(4-methoxyphenyl)aniline (1.92 g, 5.0 mmol), 1.21 g (3.26 mmol, 65 %) of a light brown oil were obtained after purification by column chromatography (silica gel, 4 x 25 cm) using hexanes/ethyl acetate 3:1 as the eluent.

R_f (hexanes/ethyl acetate 3:1): 0.36.

Maldi-TOF (POS, DCTB/$CHCl_3$ 1:3): calc: 371.163 $[M]^+$, found: 371.129.

^{1}H NMR (400.1 MHz, acetone-d_6, ppm): δ 8.16 (dd, $^{3}J_{HH}$ = 2.5 Hz, $^{4}J_{HH}$ = 0.6 Hz, 1 H), 7.66 - 7.61 (-, 3 H), 7.06 (AA‘, 4 H), 6.97 - 6.89 (-, 6 H), 6.45 (dd, $^{3}J_{HH}$ = 2.5 Hz and 1.8 Hz, 1 H), 3.79 (s, 6 H).

^{13}C NMR (100.6 MHz, acetone-d_6, ppm): δ 157.3 (C_q), 148.3 (C_q), 141.7 (C_q), 141.0 (CH), 134.7 (C_q), 127.5 (CH), 127.4 (CH), 121.6 (CH), 120.6 (CH), 115.7 (CH), 107.8 (CH), 55.8 (CH_3).

4.4 General procedure for the syntheses of *bis*-cyclometalated *μ*-chloro-bridged iridium dimers from (pyrazo-1-yl)-*N,N-bis*(4-methoxyphenyl)anilines

The appropriate (1*H*-pyrazoyl)-*N*,*N*-*bis*(*p*-methoxyphenyl)aniline (0.390 g, 1.05 mmol) and iridium(III) chloride trihydrate (0.176 g, 0.5 mmol) were dissolved in a degassed mixture of 2-ethoxyethenol and deionised water (3:1, 5 mL), sparged with nitrogen for 5 min and heated at 100 °C for 24 h. The reaction mixture was cooled down to room temperature, poured into water (100 mL) and stirred for 10 min. The flocculent precipitate was collected on a sintered glass funnel, washed successively with water, MeOH and Et_2O (10 mL each) and air-dried for 1 h.

4.4.1 (κ^2-N,C-(3-(pyrazo-1-yl)-*N,N-bis*(4-methoxyphenyl)aniline))$_4$(μ-Cl)$_2$diiridium(III) (10)

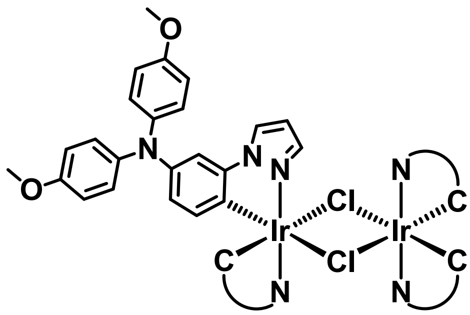

$C_{92}H_{80}Cl_2Ir_2N_{12}O_8$, M = 1937.04 g/mol

From 3-(1*H*-pyrazoyl)-*N*,*N*-*bis*(4-methoxyphenyl)aniline (0.390 g, 1.05 mmol) and iridium(III) chloride trihydrate (0.176 g, 0.50 mmol), 0.60 g (quant.) of a bright yellow-green solid were obtained. The compound was used without further purification.

MALDI-TOF (POS, DCTB : $CHCl_3$ = 1 : 3): no molecular peak was observed (m/z = 1936.486).

Fragments: [M –(C^N)$_2$IrCl]$^+$: calc. 968.243, found: 968.273;

[M –(C^N)$_2$IrCl$_2$]$^+$: calc. 933.274, found: 933.285.

4.4.2 (κ^2-N,C-(4-(pyrazo-1-yl)-*N,N-bis*(4-methoxyphenyl)aniline))$_4$(μ-Cl)$_2$diiridium(III) (11)

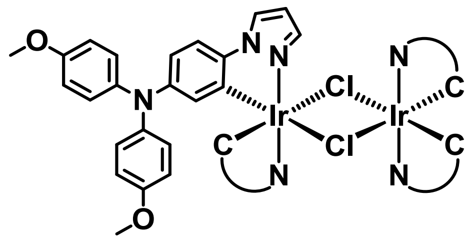

$C_{92}H_{80}Cl_2Ir_2N_{12}O_8$, M = 1937.04 g/mol

From 4-(1*H*-pyrazoyl)-*N*,*N*-*bis*(4-methoxyphenyl)aniline (0.390 g, 1.05 mmol) and iridium(III) chloride trihydrate (0.176 g, 0.50 mmol), 0.60 g (quant.) of a brown solid were obtained. The compound was used without further purification.

MALDI-TOF (POS, DCTB/$CHCl_3$ = 1:3): no molecular peak was observed (m/z = 1936.486).

Fragments: [M –(C^N)$_2$IrCl]$^+$: calc. 968.243, found: 968.216;

[M –(C^N)$_2$IrCl$_2$]$^+$: calc. 933.274, found: 933.220.

4.5 General procedure for the syntheses of the phenyldipyrrinato complexes from the *bis*-cyclometalated μ-chloro-bridged iridium dimers

Meso-phenyldipyrromethane (0.047 g, 0.21 mmol) and DDQ (0.048 g, 0.21 mmol) were dissolved in dry THF (10 mL) and stirred for 1 h at room temperature. Under a stream of nitrogen, K_2CO_3 (0.50 g, excess) was added followed by the appropriate iridium dimer. The reaction mixture was heated at 60 °C for 16 h, cooled down to room temperature and adsorbed onto celite. The celite was placed on top of a celite bed (2 x 4 cm) and the whole pad eluted with CH_2Cl_2 (≈ 100 mL). The CH_2Cl_2 extract was taken to dryness on a rotavapor and the resulting residue purified by column chromatography (silica gel, 3.5 x 20 cm). The main red band was collected, solvents removed and the red solid redissolved in CH_2Cl_2 (10 mL). Hexanes (50 mL) were added and the volume slowly reduced to ≈ 10 mL under reduced pressure. The precipitate was collected on a sintered glass funnel, washed with hexanes (3 x 5 mL) and dried in *vacuo*.

4.5.1 (κ^2-N,C-(3-(pyrazo-1-yl)-*N,N-bis*(4-methoxyphenyl)aniline))$_2$(κ^2-*N,N'*(*meso*-phenyldipyrrinato)iridium(III) (2p)

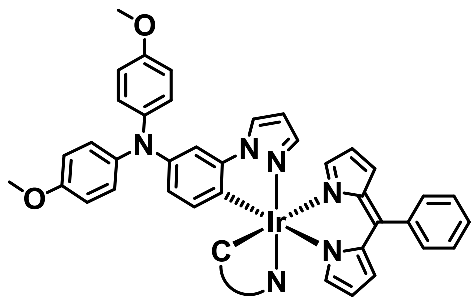

$C_{61}H_{51}IrN_8O_4$, M = 1152.33 g/mol

From (κ^2-N,C-(3-(pyrazo-1-yl)-*N,N-bis*(4-methoxyphenyl)aniline))$_4$(μ-Cl)$_2$diiridium(III) (0.193 g, 0.10 mmol) 0.20 g (0.17 mmol, 87 %) of a dark red solid were obtained. CH_2Cl_2/hexanes 4:1 (containing 1 % Et_3N) was used as the eluent for the chromatographic purification.

R_f (CH_2Cl_2/hexanes 4:1): 0.44.

Elemental analysis: calc. for $C_{61}H_{51}IrN_8O_4$: C 63.58 %, H 4.46 %, N 9.72 %,

found: C 63.33 %, H 4.44 %, N 10.15 %.

ESI (positive mode, CH_2Cl_2/MeCN 1:1): calc. 1150.36337 $[M]^+$, found : 1150.36272 (Δ =- 0.57 ppm).

^{1}H-NMR (400.1 MHz, acetone-d_6): δ 8.37 (dd, $^3J_{HH}$ = 2.9 Hz, $^4J_{HH}$ = 0.6 Hz, 2 H), 7.53 – 7.41 (-, 5 H), 7.25 (d, $^3J_{HH}$ = 2.1 Hz, 2 H), 7.12 (dd, $^3J_{HH}$ = 1.4 and 1.4 Hz, 2 H), 7.02 (dd, $^4J_{HH}$ = 2.2 Hz, $^5J_{HH}$ = 0.6 Hz, 2 H), 6.93 (AA‘, 8 H), 6.81 (BB‘, 8 H), 6.56 – 6.51 (-, 4 H), 6.44 (dd, $^3J_{HH}$ = 4.3 Hz, $^4J_{HH}$ = 1.4 Hz, 2 H), 6.33 (d, $^3J_{HH}$ = 8.0 Hz, 2 H), 6.28 (dd, $^3J_{HH}$ = 4.3 Hz, $^4J_{HH}$ = 1.4 Hz, 2 H), 3.75 (s, 12 H).

^{13}C NMR (100.6 MHz, acetone-d_6, ppm): δ 156.1 (C_q), 152.5 (CH), 149.3 (C_q), 145.7 (C_q), 144.4 (C_q), 142.8 (C_q), 140.7 (C_q), 138.5 (CH), 135.9 (C_q), 135.2 (CH), 131.6 (CH), 131.5 (CH), 131.2 (CH), 128.9 (CH), 127.9 (CH), 127.5 (1 x CH, 1 x C_q), 125.6 (CH), 122.5 (CH), 117.4 (CH), 115.4 (CH), 108.2 (CH), 55.7 (CH_3).

4.5.2 (κ^2-N,C-(4-pyrazo-1-yl)-*N,N-bis*(4-methoxyphenyl)aniline))$_2$(κ^2-*N,N'*(*meso*-phenyldipyrrinato)iridium(III) (2m)

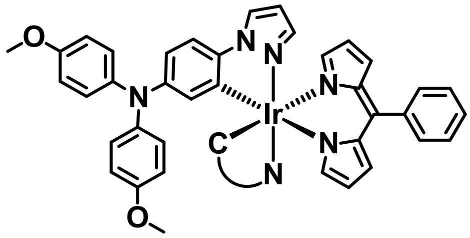

$C_{61}H_{51}IrN_8O_4$, M = 1152.33 g/mol

From (κ^2-N,C-(4-pyrazo-1-yl)-*N,N-bis*(4-methoxyphenyl)aniline)$_4$(μ-Cl)$_2$diiridium(III) (0.193 g, 0.20 mmol) 0.21 g (0.18 mmol, 91 %) of a dark red solid were obtained. A gradient from CH_2Cl_2/hexanes 4:1 to CH_2Cl_2 (containing 1 % Et_3N) was used as the eluent for the chromatographic purification.

R$_f$ (CH_2Cl_2/hexanes 4:1): 0.26.

Elemental analysis: calc. for $C_{61}H_{51}IrN_8O_4$: C 63.58 %, H 4.46 %, N 9.72 %;

Found: C 63.82 %, H 4.46 %, N 9.36 %.

ESI (positive mode, CH_2Cl_2/MeCN 1:1): calc. 1150.36337 $[M]^+$, found : 1150.36390 (Δ = 0.46 ppm).

^{1}H-NMR (400.1 MHz, acetone-d_6, ppm): δ 8.15 (dd, $^3J_{HH}$ = 2.9 Hz, $^4J_{HH}$ = 0.7 Hz, 2 H), 7.51 – 7.40 (-, 5 H), 7.33 (d, $^3J_{HH}$ = 8.5 Hz, 2 H), 7.19 (dd, $^3J_{HH}$ = 1.4 and 1.4 Hz, 2 H), 6.86 (AA', 8 H), 6.80 (BB', 8 H), 6.77 (dd, $^4J_{HH}$ = 2.2 Hz, $^5J_{HH}$ = 0.7 Hz, 2 H), 6.48 (dd, $^3J_{HH}$ = 8.5 Hz, $^4J_{HH}$ = 2.5 Hz, 2 H), 6.43 (dd, $^3J_{HH}$ = 4.3 Hz, $^3J_{HH}$ = 1.4 Hz, 2 H), 6.29 (dd, $^3J_{HH}$ = 4.3 Hz, $^4J_{HH}$ = 1.4 Hz, 2 H), 6.26 (dd, $^3J_{HH}$ = 2.8 Hz, $^3J_{HH}$ = 2.3 Hz, 2 H), 5.95 (d, $^3J_{HH}$ = 2.4 Hz, 2 H), 3.78 (s, 12 H).

^{13}C-NMR (150.9 MHz, chloroform-d_1, ppm): δ 155.1 (C$_q$), 152.4 (CH), 148.4 (C$_q$), 146.1 (C$_q$), 141.8 (C$_q$), 139.8 (C$_q$), 139.3 (C$_q$), 138.6 (C$_q$), 137.0 (CH), 135.1 (C$_q$), 130.9 (CH), 130.6 (CH), 128.0 (CH), 127.4 (CH), 127.0 (CH), 125.8 (CH), 124.3 (CH), 116.5 (CH), 114.5 (CH), 114.4 (CH), 110.6 (CH), 106.4 (CH), 55.7 (CH_3).

4.6 General procedure for the syntheses of the *meso*-naphtalene diimide dipyrrinato complexes from the *bis*-cyclometalated *μ*-chloro bridged iridium dimers

DDQ (0.030 g, 0.132 mmol) and *meso*-(4-(*N*-(2,5-di-*tert*-butylphenyl)-naphthalene-1,4,5,8-tetracarboxyldiimide)phenyl)dipyrromethane (0.081 g, 0.120 mmol) were dissolved dry THF (20 mL) and stirred for 3 h at room temperature. Under a stream of nitrogen, K_2CO_3 (0.75 g, excess) was added followed by the appropriate iridium dimer (0.116, 0.060 mmol). The reaction mixture was refluxed for 12 h, cooled down to room temperature and taken to dryness. The crude solid was taken-up in CH_2Cl_2 (25 mL) and filtered through a pad of celite (2 x 4 cm). The celite pad was washed with additional CH_2Cl_2 (≈ 100 mL) and the solvent removed from the organic extract. The resulting residue was purified by a combination of chromatographic techniques and reprecipitation from mixed-solvent systems.

4.6.1 (*κ*²-N,C-(3-(pyrazo-1-yl)-*N,N*-*bis*(4-methoxyphenyl)aniline))₂(*κ*²-*N,N'*(*meso*-(4-(*N*-(2,5-di-*tert*-butylphenyl)-naphthalene-1,4,5,8-tetracarboxyldiimide)phenyl)dipyrrinato)iridium(III) (1p)

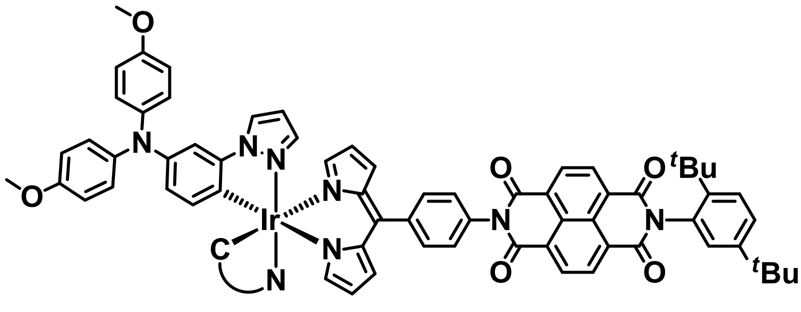

$C_{89}H_{75}IrN_{10}O_8$, M = 1604.83 g/mol

From (*κ*²-N,C-(3-(pyrazo-1-yl)-*N,N*-*bis*(4-methoxyphenyl)aniline))₄(*μ*-Cl)₂diiridium(III) (0.116 g, 0.060 mmol) 0.056 g (0.035 mmol, 29 %) of a red solid were obtained. The crude mixture was first purified by chromatography (silica gel, 4 x 25 cm) using 0.5 % ethyl acetate in CH_2Cl_2 as the eluent, followed by GPC with $CHCl_3$ as the eluent. A second flash chromatography on silica gel (3.5 x 20 cm) using 0.1 % MeOH in CH_2Cl_2 was then performed, the main red band was collected and taken to dryness. Reprecipitation of the residue from toluene/hexanes afforded the desired complex as a red solid, which was collected on a sintered glass funnel, washed with hexanes and dried *in vacuo*.

R$_f$ (CH_2Cl_2/ethyl acetate = 99.5:0.5): 0.50.

Elemental analysis: calc. for $C_{89}H_{75}IrN_{10}O_8$: C 66.61 %, H 4.71 %, N 8.73 %;

Found: C 66.09 %, H 5.00 %, N 8.35 %.

ESI (positive mode, CH_2Cl_2/MeCN 1:1): calc.1602.53698 $[M]^+$; found : 1602.53783 (Δ = 0.53 ppm).

^{1}H-NMR (600.1 MHz, chloroform-*d*, ppm): δ 8.89 (-, 4 H), 7.78 (dd, $^3J_{HH}$ = 2.9 Hz, $^4J_{HH}$ = 0.6 Hz, 2 H), 7.67 (AA‘, 2 H), 7.62 (d, $^3J_{HH}$ = 8.7 Hz, 1 H), 7.50 (dd, $^3J_{HH}$ = 8.6 Hz, $^4J_{HH}$ = 2.2 Hz, 1 H), 7.38 (BB‘, 2 H), 7.16 (m, 2 H), 7.02 (-, 9 H), 6.97 (dd, $^3J_{HH}$ = 2.2 Hz, $^4J_{HH}$ = 0.6 Hz, 2 H), 6.95 (d, $^4J_{HH}$ = 2.2 Hz, 2 H), 6.80 (BB‘, 8 H), 6.67 (dd, $^3J_{HH}$ = 4.3 Hz, $^4J_{HH}$ = 1.3 Hz, 2 H), 6.56 (dd, $^3J_{HH}$ = 8.0 Hz, $^4J_{HH}$ = 2.2 Hz, 2 H), 6.37 - 6.35 (-, 4 H), 6.27 (d, $^3J_{HH}$ = 8.0 Hz, 2 H), 3.78 (s, 12 H), 1.34 (s, 9 H), 1.29 (s, 9 H).

^{13}C-NMR (150.9 MHz, chloroform-*d*, ppm): δ 164.0 (C_q), 163.2 (C_q), 155.1 (C_q), 152.5 (CH), 150.6 (C_q), 147.1 (C_q), 144.5 (C_q), 143.8 (C_q), 143.3 (C_q), 142.1 (C_q), 140.8 (C_q), 137.7 (CH), 135.1 (C_q), 134.5 (CH), 134.4 (C_q), 132.1 (C_q), 131.8 (CH), 131.7 (CH), 131.6 (CH), 131.3 (CH), 130.1 (C_q), 129.2 (CH), 127.7 (CH), 127.51 (C_q), 127.47 (C_q), 127.40 (C_q), 127.36 (CH), 127.2 (C_q), 126.9 (CH), 125.4 (CH), 125.2 (CH), 121.3 (CH), 116.9 (CH), 114.7 (CH), 107.0 (CH), 106.5 (CH), 55.7 (CH_3), 35.7 (C_q), 34.5 (C_q) 31.9 (CH_3), 31.4 (CH_3).

4.6.2 (κ^2-N,C-(4-(pyrazo-1-yl)-*N,N-bis*(4-methoxyphenyl)aniline))$_2$(κ^2-*N,N'*(*meso*-(4-(*N*-(2,5-di-*tert*-butylphenyl)-naphthalene-1,4,5,8-tetracarboxyldiimide)phenyl)dipyrrinato)iridium(III) (1m)

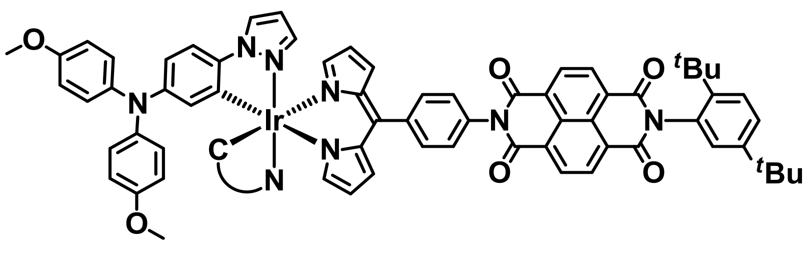

$C_{89}H_{75}IrN_{10}O_8$, M = 1604.83 g/mol

From (κ^2-N,C-(4-(pyrazo-1-yl)-*N,N-bis*(4-methoxyphenyl)aniline))$_4$(μ-Cl)$_2$ diiridium(III) (0.116 g, 0.060 mmol) 0.120 g (0.075 mmol, 62 %) of a red solid were obtained. The crude mixture was first purified by chromatography (silica gel, 4 x 25 cm) using a gradient of CH_2Cl_2/ethyl acetate

99.5:0.5 → 99:1 → 98:2 as the eluent, followed by GPC with $CHCl_3$ as the eluent. Reprecipitation of the residue from CH_2Cl_2/hexanes afforded the desired complex as a red solid, which was collected on a sintered glass funnel, washed with hexanes and dried *in vacuo*.

R_f (CH_2Cl_2/ethyl acetate = 99.5:0.5): 0.38

Elemental analysis: calc. for $C_{89}H_{75}IrN_{10}O_8$: C 66.61 %, H 4.71 %, N 8.73 %;

Found: C 66.43 %, H 4.76 %, N 8.42 %..

ESI (positive mode, CH_2Cl_2/MeCN 1:1): calc.1602.53698 $[M]^+$; found : 1602.53815 (Δ = 0.73 ppm).

^{1}H NMR (600.1 MHz, chloroform-*d*, ppm): δ 8.89 (-, 4 H), 7.67 (AA‘, 2 H), 7.63 - 7.61 (-, 3 H), 7.50 (dd, $^3J_{HH}$ = 8.6 Hz, $^4J_{HH}$ = 2.2 Hz, 1 H), 7.37 (BB‘, 2 H), 7.24 (dd, $^3J_{HH}$ = 1.3 Hz and 1.3 Hz, 2 H), 7.03 (d, $^4J_{HH}$ = 2.2 Hz, 1 H), 6.98 (d, $^3J_{HH}$ = 8.5 Hz, 2 H), 6.89 (AA‘, 8 H), 6.78 (dd, $^3J_{HH}$ = 2.2 Hz, $^4J_{HH}$ = 0.6 Hz, 2 H), 6.74 (BB‘, 8 H), 6.66 (dd, $^3J_{HH}$ = 4.3 Hz, $^4J_{HH}$ = 1.3 Hz, 2 H), 6.54 (dd, $^3J_{HH}$ = 8.5 Hz, $^4J_{HH}$ = 2.5 Hz, 2 H), 6.35 (dd, $^3J_{HH}$ = 4.3 Hz, $^4J_{HH}$ =1.3 Hz, 2 H), 6.13 - 6.11 (-, 2H), 5.82 (d, $^4J_{HH}$ = 2.5 Hz, 2 H), 3.80 (s, 12 H), 1.34 (s, 9 H), 1.29 (s, 9 H).

^{13}C NMR (150.9 MHz, chloroform-*d*, ppm): δ 164.0 (C_q), 163.1 (C_q), 155.1 (CH), 152.8 (CH), 150.6 (C_q), 147.1 (C_q), 146.1 (C_q), 143.8 (C_q), 141.8 (C_q), 140.7 (C_q), 139.1 (C_q), 138.6 (C_q), 137.0 (CH), 134.9 (C_q), 134.4 (C_q), 132.1 (C_q), 131.8 (CH), 131.7 (CH), 131.6 (CH), 131.1 (CH), 129.2 (CH), 127.7 (CH), 127.50 (C_q), 127.46 (C_q), 127.4 (C_q), 127.34 (CH), 127.32 (C_q), 127.2 (C_q), 126.9 (CH), 125.8 (CH), 124.4 (CH), 116.9 (CH), 114.5 (CH), 114.4 (CH), 110.7 (CH), 106.5 (CH), 55.7 (CH_3), 35.7 (C_q), 34.4 (C_q), 31.9 (CH_3), 31.4 (CH_3).

B. Electrochemistry

All electrochemical measurements were realised in CH_2Cl_2 with tetrabutylammonium hexafluorophosphate [*n*-Bu_4N][PF_6] (0.2 M) as supporting electrolyte. CH_2Cl_2 was first dried over calcium chloride, distilled from calcium hydride and stored over activated alumina prior to use. [*n*-Bu_4N][PF_6] was synthesised according to literature,[11] recrystallised from ethanol/water and dried in high vacuum.

1. Cyclic Voltammetry

Cyclic voltammograms were recorded on a Gamry Reference 600 potentiostat and a three electrode setup with a platinum disc working electrode (Ø = 1 mm), a platinum wire counter electrode and a leak free Ag/AgCl reference electrode (Warner Instruments, Hamden, CT, USA). The cell was oven dried and flushed with argon before use. All voltammograms were referenced to the ferrocene / ferrocenium (Fc/Fc^+) redox couple, the potentials are listed in Table S1.

The recorded voltammograms were analysed and fitted with DigiElch Software (Gamry, version 6.F, build 3.005).

Table S1. Cyclic voltammetry of **1m**, **2m, 1p** and **2p** (1 – 5 mM) in 0.2 M [*n*-Bu_4N][PF_6]/CH_2Cl_2 , at v = 250 mV s^{-1} vs. Fc/Fc^+.

compound	$E^{Red}_{1/2}$ / mV (dipy)	$E^{Red}_{1/2}$ / mV (NDI_2)	$E^{Red}_{1/2}$ / mV (NDI_1)	$E^{Ox}_{1/2}$ / mV (TAA_1)	$E^{Ox}_{1/2}$ / mV (TAA_2)	E^{Ox}_{pa} / mV (dipy)	$\Delta E_{1/2}$ / mV
2p	- 2035^{i}	–	–	1^{r,f}	160^{r,f}	640^{i}	1881
2m	- 1995^{i}	–	–	71^{r}	162^{r}	635^{i}	1961
1p	- 1945^{i,a}	- 1485^{r}	- 1015^{r}	8^{r,f}	161^{r,f}	650^{i}	1023
1m	- 1940^{i,a}	- 1485^{r}	- 1010^{r}	72^{r,f}	163^{r,f}	660^{i}	1082

i = irreversible, r = reversible, f = determined by fitting, a = values in MeCN (distilled over CaH_2, with a 0.1 M [*n*-Bu_4N][PF_6]/MecN solution, scan rate of 250 mV s^{-1}, vs. Fc/Fc^+.

2. Spectroelectrochemistry (SEC)

UV/vis/NIR-spectroelectrochemistry was performed at rt in a custom built three electrode quartz-cell sample compartment implemented in a Jasco V-670 spectrometer. The cell consists of a platinum disc working electrode (Ø = 6 mm), a gold covered stainless steel (V2A) plate as counter electrode and an AgCl-covered silver wire as pseudo-reference electrode.[12] All experiments were measured in reflexion with a path length of 100 μm. The working electrode potential was controlled by a Princeton Applied Research Model 283 potentiostat (20 or 50 mV steps). The concentration of **2p, 2m** and **NDI** was $8.68\cdot10^{-4}$ - $1.73\cdot10^{-3}$ mol l^{-1}. The spectra of "pure" radical anion **6**$^{-}$ and dianion **6**$^{2-}$ were obtained by subtracting the spectra of neutral **6** from the spectra measured for the potential for the first and second reduction process (Figure S3). The cation **2p/m⁺** and dication **2p/m²⁺** spectra were deconvoluted with SpecFit Software[13], due to overlapping redox processes at positive potential (Figure 2a and 2c). The resulting spectra for **6**$^-$, **2p/m**$^+$ and the sum of both radical ions are shown in Figure S1 and S2, and are in very good agreement with the transient signal for **1p** and **1m** (see fs-transient absorption).

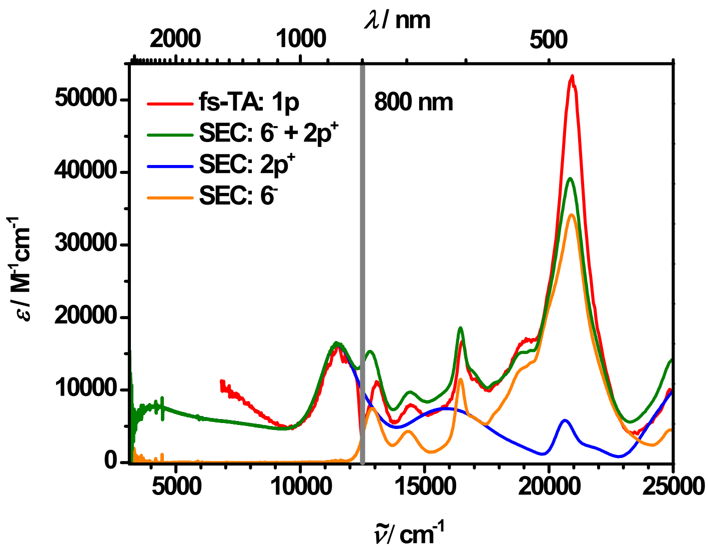

Figure S1. SEC of **2p** and **6** in CH_2Cl_2: spectra of both first reduction of **6** (orange) and first oxidation of **2p** (blue) and sum of the **6**$^-$ and **2p**$^+$ spectra (green). For comparison the fs-transient absorption spectra of the CS state of **1p** is plotted in red. The grey bar covers the central wavelength of the laser fundamental at 12 500 cm^{-1} (800 nm).

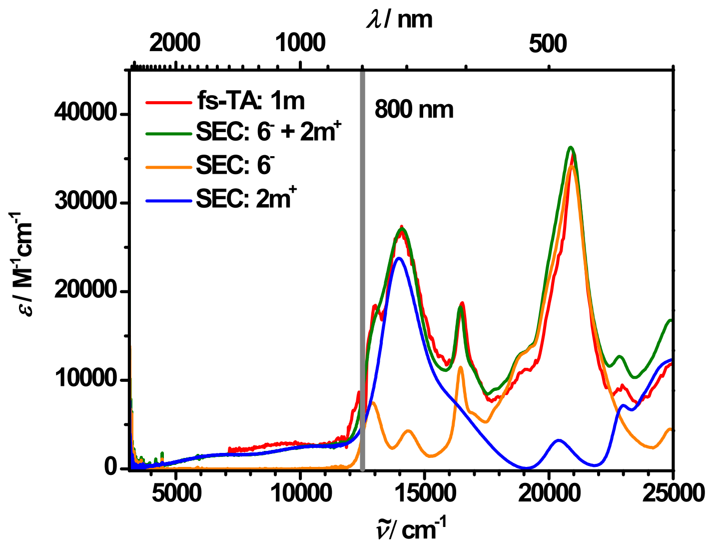

Figure S2. SEC of **2m** and **6** in CH_2Cl_2: spectra of both first reduction of **6** (orange) and first oxidation of **2m** (blue) and sum of the **6**$^-$ and **2m**$^+$ spectra (green). For comparison the fs-transient absorption spectra of the CS state of **1m** is plotted in red. The grey bar covers the central wavelength of the laser fundamental at 12 500 cm^{-1} (800 nm).

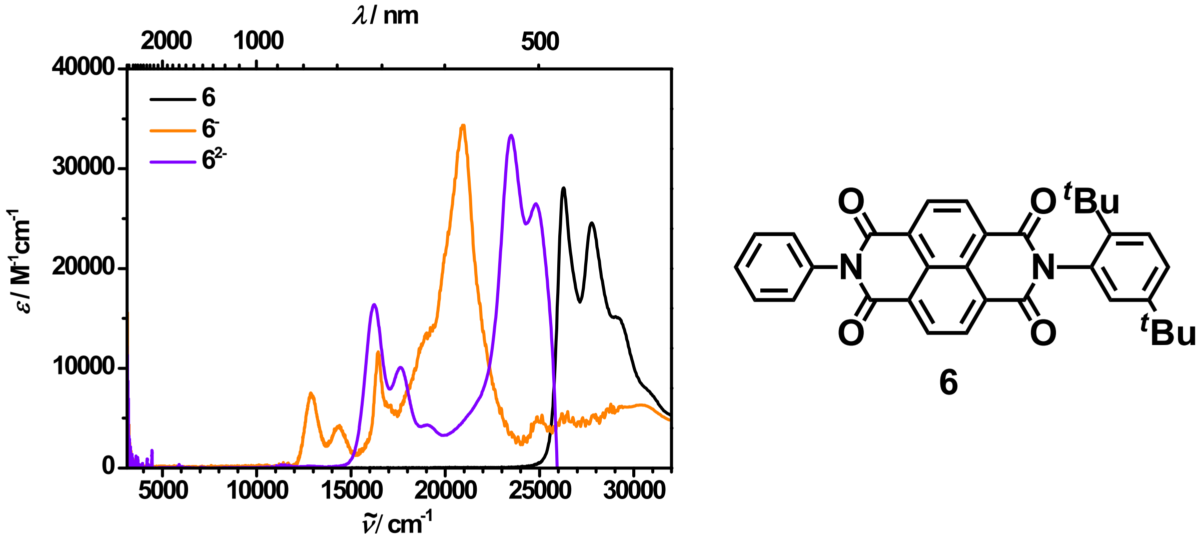

Figure S3. SEC of **6** in CH_2Cl_2: spectra of neutral species (black), first and second reduction (orange and purple, respectively).

C. UV/vis spectroscopy

All solvents were of spectroscopic grade and were used without further purification. Absorption spectra were recorded with a JASCO V-670 UV/vis/NIR spectrometer in 1 cm quartz cuvettes from Starna (Pfungstadt, Germany) at rt.

D. Femtosecond transient-absorption spectroscopy

The pump-probe experiments were performed in a 2 mm quartz cuvette equipped with a micro-stir bar. The compounds were dissolved in Uvasol® solvents from Merck to a concentration that the optical density is of 0.25 – 0.35 at the excitation energy, were filtered and purged with argon for 15 min. The laser system consists of an ultrafast Ti:Sapphire amplifier (Newport-Spectra-Physics, Solstice) with a fundamental wavenumber of 12 500 cm^{-1} (800 nm), a pulse length of 100 fs and a repetition rate of 1 kHz. One part of the output power was used to seed an optical parametric amplifier (Newport-Spectra-Physics, TOPAS) as the source for the pump pulse with an pump energy of 100 nJ, a wavenumber of 20 800 cm^{-1} (480 nm) and a pulse length of 140 fs. A small fraction of the Ti:sapphire output was focused into a moving calcium fluoride-plate (vis) / Ti:sapphire crystal (NIR) to produce a white light continuum in the visible between 25 000 cm^{-1} (400 nm) and 11 800 cm^{-1} (850 nm) and in the NIR between 11 800 cm^{-1} (850 nm) and 6 820 cm^{-1} (1466 nm), respectively. The resulting white light acted as the probe pulse and was horizontally polarised. The measurements were done under magic angle conditions and the excitation pulse was collimated to a spot, which was at least 2 times larger than the diameter of the spatially overlapping probe pulse. After passing the sample the probe pulses were detected *via* a transient absorption spectrometer (Ultrafast Systems, Helios) with a CMOS (1.5 nm intrinsic resolution, 350 – 860 nm sensitivity range) sensor and an InGaAs (3.5 nm intrinsic resolution, 800 – 1600 nm sensitivity range) sensor, respectively. Part of the probe light pulse was used to correct for intensity fluctuations of the white light continuum. A mechanical chopper, working at 500 Hz, blocked every second pulse, in order to measure I and I_0, thus enabling low noise-to-shot-measurements. The photoinduced change in optical density can directly be recorded by comparing the transmitted spectral intensity of consecutive pulses [$I(\lambda, \tau)$, $I_0(\lambda)$]:

$$\Delta OD = -\log\left[\frac{I(\lambda,\tau)}{I_0(\lambda)}\right]$$

The relative temporal delay between pump and probe pulses was varied over a maximum range of 8 ns with a motorised, computer-controlled linear stage. For small delay times, the delay interval between two consecutive data points was 20 fs and was increased up to 200 ps for very large delay times. The stability of the samples was verified by recording the absorption spectra before and after the time-resolved measurements.

The time resolved spectra were analysed by global fitting with GLOTARAN (v. 1.2)[14]. For this purpose a sequential model (i. e. unbranched unidirectional model) was applied to model the white light dispersion (chirp), a Gaussian type IRF and the coherent artefact at the time zero to yield the evolution associated spectra (EAS) and their corresponding time constants. The white light dispersion (chirp) was corrected by fitting a third order polynomial to the crossphase modulation signal of the pure solvent under otherwise identical experimental conditions. Singular value decomposition was used to estimate the number of components and the quality of the fits.

For the dual probe alignment (sample/reference), each pair of laser pulses was normalised to the linear absorption spectra, after acquiring a certain number of transient spectra:

$$\Delta A = \log\left[\left(\frac{I_{ex}(\text{sample})}{I_0(\text{sample})}\right)\left(\frac{I_{ex}(\text{reference})}{I_0(\text{reference})}\right)\right]$$

I_{ex} (sample): intensity of the probe light after the sample when the excitation light was incident on the sample

I_{ex} (reference): intensity of light in the reference channel when the excitation light was incident on the sample

I_0 (sample): intensity of probe light after the sample when the excitation light was blocked by optical chopper

I_0 (reference): intensity of light in the reference channel when the excitation light was blocked by optical chopper

Assuming the splitting ratio between the sample and the reference probe beam to be constant, reflection of the fluctuations in the sample beam by the corresponding fluctuations in the reference beam are not related to the excitation pulse. This method is used mainly with less stable white light.

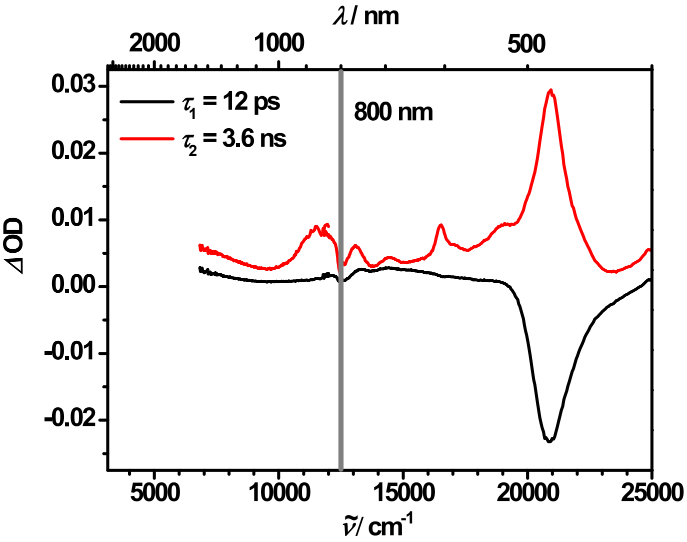

Figure S4. Species associated difference spectra (EADS) of **1m** from a global target analysis of a transient map obtained by 480 nm excitation in CH_2Cl_2. The grey bar covers the central wavelength of the laser fundamental at 12 500 cm^{-1} (800 nm).

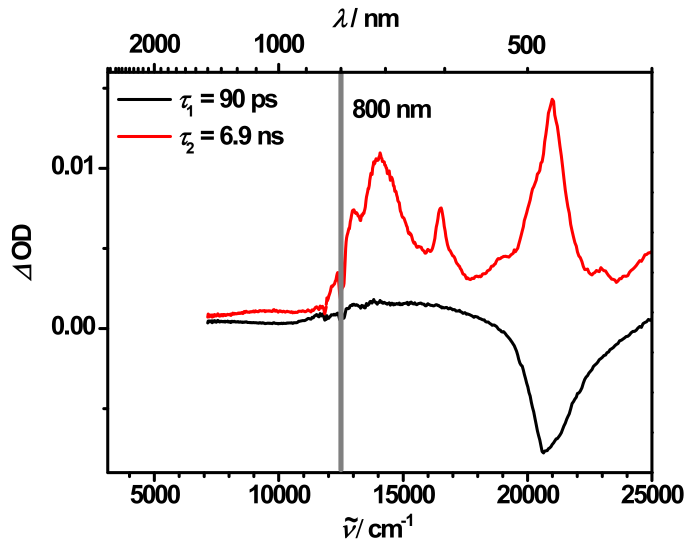

Figure S5. Species associated difference spectra (EADS) of **1p** from a global target analysis of a transient map obtained by 480 nm excitation in CH_2Cl_2. The grey bar covers the central wavelength of the laser fundamental at 12 500 cm^{-1} (800 nm).

E. DFT-calculations

The charge-separated state was simulated by calculating the single oxidised dyads **2p** and **2m**. Structure optimizations of the single oxidised species were performed analogously to the method described by Kaupp et al. for MV compounds with *bis*(triarylamine) motifs[15]. A preliminary conformational analysis was done with the ORCA software package[16] and the BLYP35 functional (by using the BHandHLYP keyword and subsequently setting the HF part to 35% in the method block, ACM_A = 0.35, ACM_B = 0.65) in combination with the COSMO[17] solvent model for dichloromethane. As basis sets def2-SVP were used for H, C, O, and N and def2-TZVP for Ir.[18] In addition ECP of the Stuttgart-Dresden group were applied for Ir.[19] Symmetric conformations were used as starting structures but the optimisation was done without any symmetry constraints. To include dispersion corrections in the optimisation the D3BJ keyword was applied in combination with the following coefficents: D3S6 = 1.000, D3A1 = 0.2793, D3S8 = 1.0354, D3A2 = 4.9615. The coefficients are in fact the values for BHLYP and were not further optimized for BLYP35. To increase calculation speed the chain-of-spheres approximation (RIJCOSX) was used.[20]

Only the energetically lowest conformations found for the complexes were further investigated. TDDFT-calculations for the oxidised complexes were performed with Gaussian09 Revision D.01.[21] All calculations were done using the BLYP35 functional with 35% HF exchange (BLYP in combination with IOP(3/76=0650003500), IOP(3/77=1000010000), and IOP(3/78=1000010000)) and the above mentioned basis set and ECP combination (taken from the EMSL database[22]). As a solvent model the C-PCM[23] method was applied with dichloromethane as solvent. Spin densities of the ground states of **2p⁺** and **2m⁺** and the electron density difference (EDD) plots were calculated with Gaussian09. The cube files were visualized with Avogadro[24] (isovalue of 0.002 for the spin densities and for the EDD plots) and rendered with PovRay.

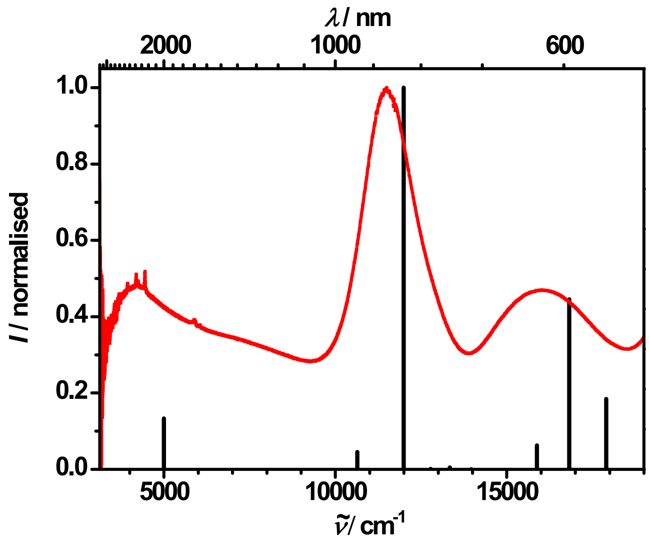

Figure S6. Absorption spectrum and stick diagram of the computed transitions of the monocation of **2p** (see Table S2 for exact energies and oscillator strengths).

Table S2. Transition energies and oscillator strengths (f) of the computed transitions of the single oxidised complex **2p**.

λ / nm	*f* / a. u.	$\tilde{\nu}$ / cm^{-1}
457.1	0.0002	21877
457.6	0.0013	21853
459.6	0.0012	21758
462.7	0.0004	21612
492.4	0.0086	20309
519.6	0.0098	19246
558.6	0.0686	17902
594.4	0.1656	16824
629.7	0.0232	15881
716.7	0.0000	13953
749.7	0.0018	13339
782.7	0.0004	12776
833.9	0.3717	11992
939.7	0.0169	10642
2000.7	0.0496	4998

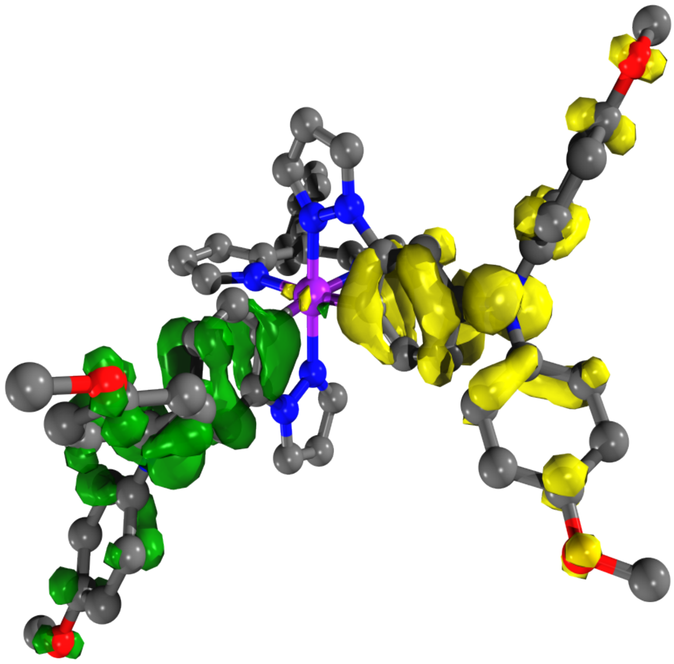

Figure S7. Electron density difference plot (isovalue: ±0.002, yellow = lowered electron density, green = increased electron density) of the calculated transition of **2p⁺** at 4998 cm^{-1} (2001 nm) with f = 0.0496.

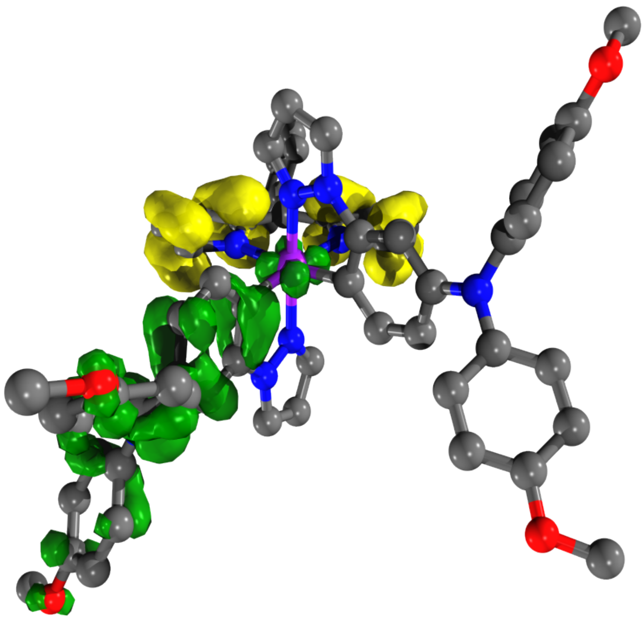

Figure S8. Electron density difference plot (isovalue: ±0.002, yellow = lowered electron density, green = increased electron density) of the calculated transition of **2p⁺** at 10642 cm^{-1} (839.7 nm) with f = 0.0169.

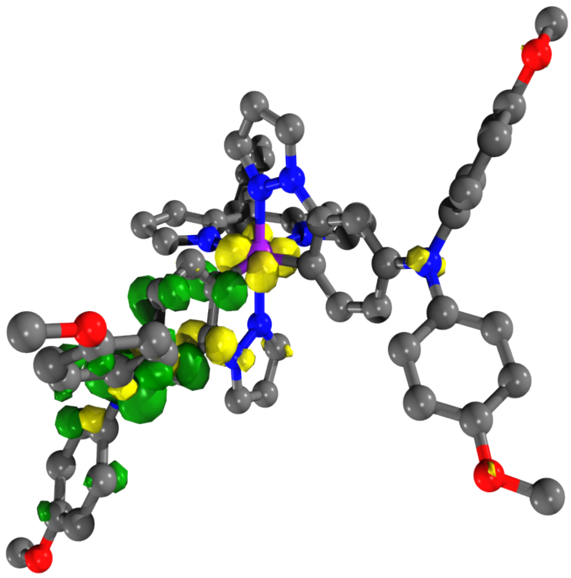

Figure S9. Electron density difference plot (isovalue: ±0.002, yellow = lowered electron density, green = increased electron density) of the calculated transition of **2p⁺** at 11992 cm^{-1} (833.9 nm) with f = 0.3717.

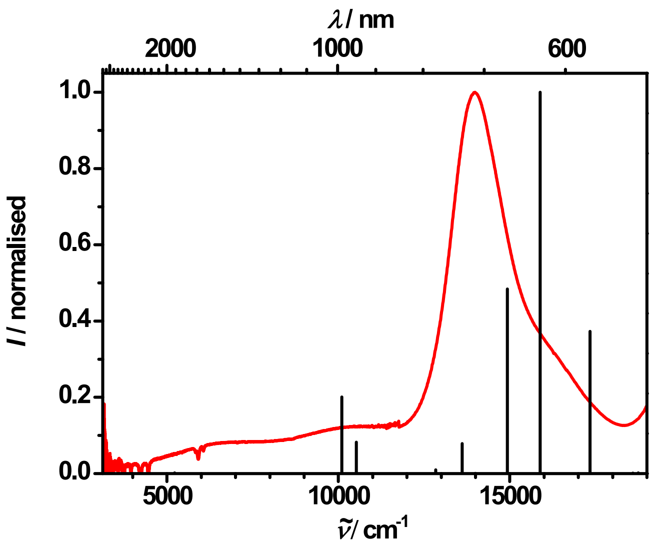

Figure S10. Absorption spectrum and stick diagram of the computed transitions of the monocation of **2m** (see Table S3 for exact energies and oscillator strengths).

Table S3. Transition energies and oscillator strengths (f) of the computed transitions of the single oxidised complex **2m**.

λ / nm	*f* / a. u.	$\tilde{\nu}$ / cm^{-1}
426.6	0.0026	23441
433.6	0.0000	23063
434	0.0009	23042
436.6	0.0116	22904
443.8	0.0000	22533
445	0.0004	22472
452.9	0.0043	22080
466.1	0.0000	21455
474.1	0.0000	21093
533.4	0.0005	18748
538	0.0003	18587
576.8	0.1047	17337
629.5	0.2806	15886
669.8	0.1358	14930
714.5	0.0001	13996
734.7	0.0221	13611
779.1	0.0028	12835
950.2	0.0231	10524
990.2	0.0564	10099
1916.0	0.0005	5219

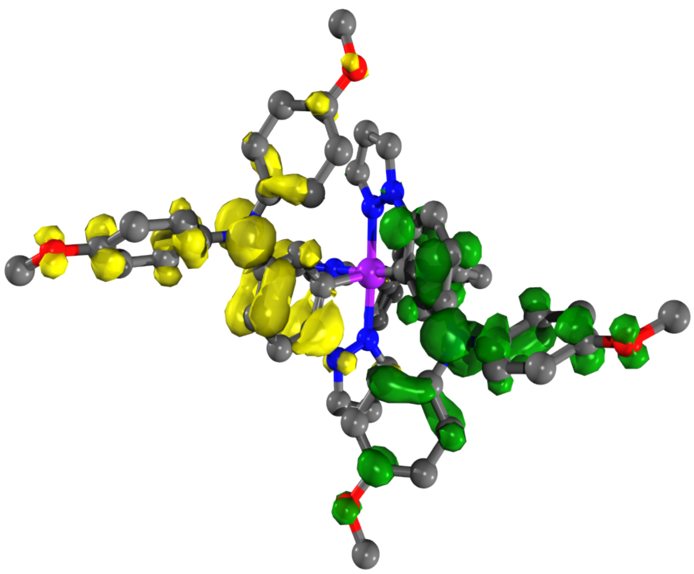

Figure S11. Electron density difference plot (isovalue: ±0.002, yellow = lowered electron density, green = increased electron density) of the calculated transition of **2m^{+}** at 5219 cm^{-1} (1920 nm) with f = 0.0005.

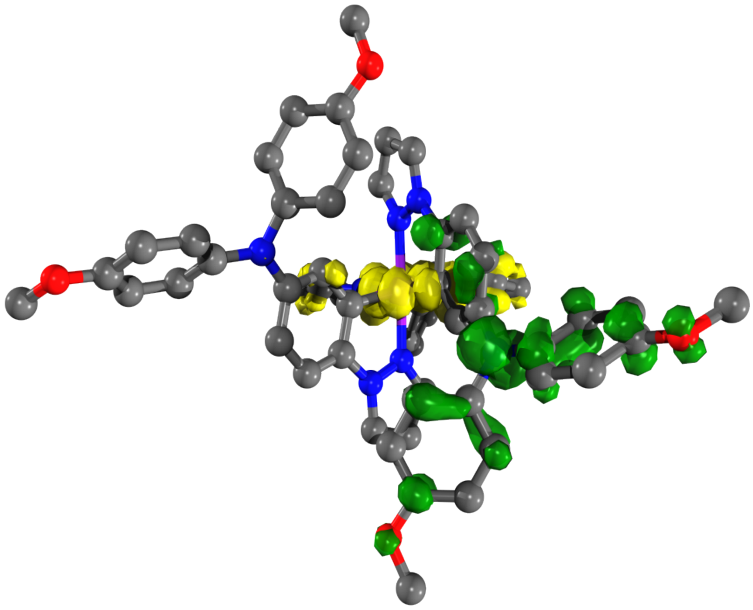

Figure S12. Electron density difference plot (isovalue: ±0.002, yellow = lowered electron density, green = increased electron density) of the calculated transition of **2m⁺** at 10099 cm^{-1} (990.2 nm) with f = 0.0564.

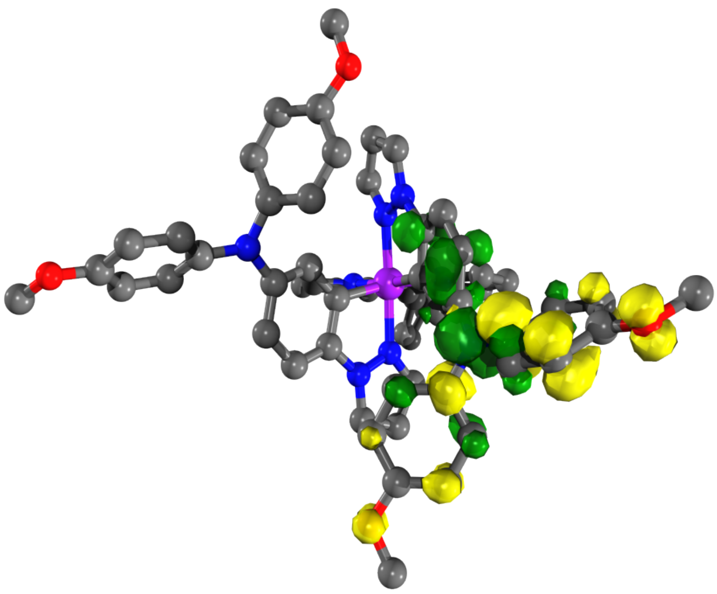

Figure S13. Electron density difference plot (isovalue: ±0.002, yellow = lowered electron density, green = increased electron density) of the calculated transition of **2m⁺** at 15886 cm^{-1} (629.5 nm) with f = 0.2806.

[1] D. F. Shriver, Drezdon M. A. , *The manipulation of air-sensitive compounds.*, Ed., John Wiley & Sons, New York, **1986**.

[2] W. C. Still, M. Kahn, A. Mitra, *J. Org. Chem.* **1978**, *43*, 2923-2925.

[3] G. R. Fulmer, A. J. M. Miller, N. H. Sherden, H. E. Gottlieb, A. Nudelman, B. M. Stoltz, J. E. Bercaw, K. I. Goldberg, *Organometallics* **2010**, *29*, 2176-2179.

[4] A. K. C. Mengel, B. He, O. S. Wenger, *J. Org. Chem.* **2012**, *77*, 6545-6552.

[5] R. W. Boyle, C. Bruckner, J. Posakony, B. R. James, D. Dolphin, *Org. Synth.* **1999**, *76*, 287-293.

[6] J. H. Klein, T. L. Sunderland, C. Kaufmann, M. Holzapfel, A. Schmiedel, C. Lambert, *Phys. Chem. Chem. Phys.* **2013**, *15*, 16024-16030.

[7] R. J. Bushby, D. R. McGill, K. M. Ng, N. Taylor, *J. Chem. Soc.-Perkin Trans. 2* **1997**, 1405-1414.

[8] H. J. Cristau, P. P. Cellier, J. F. Spindler, M. Taillefer, *Eur. J. Org. Chem.* **2004**, 695-709.

[9] K. Hanson, A. Tamayo, V. V. Diev, M. T. Whited, P. I. Djurovich, M. E. Thompson, *Inorg. Chem.* **2010**, *49*, 6077-6084.

[10] M. Nonoyama, *Bull. Chem. Soc. Jpn.* **1974**, *47*, 767-768.

[11] S. E. Dummling, E.; Schneider, S.; Speiser, B.; Wuerde, M., *Curr. Sep. Drug Dev.* **1996**, *15*, 53-56.

[12] S. Amthor, C. Lambert, *J. Phys. Chem. A* **2006**, *110*, 1177-1189.

[13] Specfit/32™ V3.0.23, Program for Multivariate Data Analysis, Spectrum Software Associates, Marlborough (USA), 1993.

[14] I. H. M. van Stokkum, D. S. Larsen, R. van Grondelle, *Biochim. Biophys. Acta-Bioenerg.* **2004**, *1657*, 82-104.

[15] a) M. Kaupp, M. Renz, M. Parthey, M. Stolte, F. Würthner, C. Lambert, *Phys. Chem. Chem. Phys.* **2011**, *13*, 16973-16986; b) M. Parthey, K. B. Vincent, M. Renz, P. A. Schauer, D. S. Yufit, J. A. K. Howard, M. Kaupp, P. J. Low, *Inorg. Chem.* **2014**, *53*, 1544-1554.

[16] a) F. Neese, F. Wennmohs, U. Becker, D. Bykov, D. Ganyushin, A. Hansen, R. Izsák, D. G. Liakos, C. Kollmar, S. Kossmann, D. A. Pantazis, T. Petrenko, C. Reimann, C. Riplinger, M. Roemelt, B. Sandhöfer, I. Schapiro, K. Sivalingam, B. Wezisla, version 3.0.2 ed., Max Planck Institute for Chemical EnergyConversion, Germany, **2014**; b) F. Neese, *Wiley Interdisciplinary Reviews: Computational Molecular Science* **2012**, *2*, 73-78.

[17] A. Klamt, *Wiley Interdiscip. Rev.-Comput. Mol. Sci.* **2011**, *1*, 699-709.

[18] F. Weigend, R. Ahlrichs, *Phys. Chem. Chem. Phys.* **2005**, *7*, 3297-3305.

[19] D. Andrae, U. Häußermann, M. Dolg, H. Stoll, H. Preuß, *Theor. Chim. Acta* **1990**, *77*, 123-141.

[20] a) F. Neese, F. Wennmohs, A. Hansen, U. Becker, *Chem. Phys.* **2009**, *356*, 98-109; b) R. Izsak, F. Neese, *The Journal of Chemical Physics* **2011**, *135*, 144105-144111.

[21] M. J. Frisch, G. W. Trucks, H. B. Schlegel, G. E. Scuseria, M. A. Robb, J. R. Cheeseman, G. Scalmani, V. Barone, B. Mennucci, G. A. Petersson, H. Nakatsuji, M. Caricato, X. Li, H. P. Hratchian, A. F. Izmaylov, J. Bloino, G. Zheng, J. L. Sonnenberg, M. Hada, M. Ehara, K. Toyota, R. Fukuda, J. Hasegawa, M. Ishida, T. Nakajima, Y. Honda, O. Kitao, H. Nakai, T. Vreven, J. J. A. Montgomery, J. E. Peralta, F. Ogliaro, M. Bearpark, J. J. Heyd, E. Brothers, K. N. Kudin, V. N. Staroverov, T. Keith, R. Kobayashi, J. Normand, K. Raghavachari, A. Rendell, J. C. Burant, S. S. Iyengar, J. Tomasi, M. Cossi, N. Rega, J. M. Millam, M. Klene, J. E. Knox, J. B. Cross, V. Bakken, C. Adamo, J. Jaramillo, R. Gomperts, R. E. Stratmann, O. Yazyev, A. J. Austin, R. Cammi, C. Pomelli, J. W. Ochterski, R. L. Martin, K. Morokuma, V. G. Zakrzewski, G. A. Voth, P. Salvador, J. J. Dannenberg, S. Dapprich, A. D. Daniels, O. Farkas, J. B. Foresman, J. V. Ortiz, J. Cioslowski, D. J. Fox, revision D.01 ed., Gaussian, Inc., Wallingford CT, **2013**.

[22] K. L. Schuchardt, B. T. Didier, T. Elsethagen, L. Sun, V. Gurumoorthi, J. Chase, J. Li, T. L. Windus, *J. Chem. Inf. Model.* **2007**, *47*, 1045-1052.

[23] a) M. Cossi, N. Rega, G. Scalmani, V. Barone, *J. Comput. Chem.* **2003**, *24*, 669-681; b) V. Barone, M. Cossi, *J. Phys. Chem. A* **1998**, *102*, 1995-2001.

[24] M. Hanwell, D. Curtis, D. Lonie, T. Vandermeersch, E. Zurek, G. Hutchison, *J. Cheminf.* **2012**, *4*, 17.